

## Two-dimensional excitons in three-dimensional hexagonal boron nitride

X. K. Cao, B. Clubine, J. H. Edgar, J. Y. Lin, and H. X. Jiang

Citation: *Appl. Phys. Lett.* **103**, 191106 (2013); doi: 10.1063/1.4829026

View online: <http://dx.doi.org/10.1063/1.4829026>

View Table of Contents: <http://apl.aip.org/resource/1/APPLAB/v103/i19>

Published by the AIP Publishing LLC.

---

### Additional information on Appl. Phys. Lett.

Journal Homepage: <http://apl.aip.org/>

Journal Information: [http://apl.aip.org/about/about\\_the\\_journal](http://apl.aip.org/about/about_the_journal)

Top downloads: [http://apl.aip.org/features/most\\_downloaded](http://apl.aip.org/features/most_downloaded)

Information for Authors: <http://apl.aip.org/authors>



[www.goodfellowusa.com](http://www.goodfellowusa.com)

**Goodfellow**

metals • ceramics • polymers  
composites • compounds • glasses

**Save 5% • Buy online**

**70,000 products • Fast shipping**

## Two-dimensional excitons in three-dimensional hexagonal boron nitride

X. K. Cao,<sup>1</sup> B. Clubine,<sup>2</sup> J. H. Edgar,<sup>2</sup> J. Y. Lin,<sup>1,a)</sup> and H. X. Jiang<sup>1,b)</sup>

<sup>1</sup>Department of Electrical and Computer Engineering, Texas Tech University, Lubbock, Texas 79409, USA

<sup>2</sup>Department of Chemical Engineering, Kansas State University, Manhattan, Kansas 66506, USA

(Received 4 August 2013; accepted 21 October 2013; published online 5 November 2013)

The recombination processes of excitons in hexagonal boron nitride (hBN) have been probed using time-resolved photoluminescence. It was found that the theory for two-dimensional (2D) exciton recombination describes well the exciton dynamics in three-dimensional hBN. The exciton Bohr radius and binding energy deduced from the temperature dependent exciton recombination lifetime is around 8 Å and 740 meV, respectively. The effective masses of electrons and holes in 2D hBN deduced from the generalized relativistic dispersion relation of 2D systems are 0.54 $m_0$ , which are remarkably consistent with the exciton reduced mass deduced from the experimental data. Our results illustrate that hBN represents an ideal platform to study the 2D optical properties as well as the relativistic properties of particles in a condensed matter system. © 2013 AIP Publishing LLC. [<http://dx.doi.org/10.1063/1.4829026>]

Hexagonal boron nitride (hBN) has attracted a great deal of research interest due to its unique physical properties including high temperature and chemical stability, large thermal conductivity, and corrosion resistance, large energy band gap ( $E_g \sim 6$  eV), and large neutron capture cross section.<sup>1–9</sup> Due to its similar in-plane lattice constant to graphene and chemical inertness and resistance to oxidation, hBN is also considered as the ideal template and gate dielectric layer in graphene electronics.<sup>10–17</sup> Lasing action in deep ultraviolet (DUV) region ( $\sim 225$  nm) by electron beam pumping was demonstrated in millimeter size hBN bulk crystals,<sup>5</sup> revealing its potential for realizing semiconductor DUV light sources. More recently, the synthesis of wafer-scale semiconducting hBN epitaxial layers using metal organic chemical vapor deposition growth opens up fresh opportunities to explore hBN as an active material for DUV optoelectronic and neutron detector device applications.<sup>4,18–21</sup>

Although hBN bulk crystals and epilayers are three-dimensional (3D) systems, the optical properties of 3D hBN are expected to be similar to those of two-dimensional (2D) single layer BN.<sup>22</sup> This is due to weak Van der Waals interactions and large distance (3.33 Å) between layers in hBN. Consequently, the interlayer optical transitions are much weaker than those within the layers.<sup>22</sup> Thus, hBN provides an ideal platform to study fundamental optical and transport properties of 2D semiconductor systems. For instance, the large  $p \rightarrow p$  transition rate combined with the large joint density of states of electron-hole pairs resulting from the 2D nature of hBN lead to high emission efficiency. The band edge emission in hBN epilayers is about two orders of magnitude larger than that in AlN (Ref. 22) which is the current default material of choice for DUV photonic device fabrication.

Currently, bulk hBN crystals are in small size.<sup>5–9</sup> However, these materials possess high crystalline quality and can serve as a benchmark for the understanding of the basic optical properties as well as for the development of

wafer-size crystals of hBN. We present here the results of studies on exciton recombination dynamics in hBN bulk crystals probed by DUV time-resolved photoluminescence (PL) spectroscopy. Bulk hBN materials employed in this study were grown at ambient pressure by the flux method using a nickel (Ni) and chromium (Cr) solvent mixture.<sup>23,24</sup> High purity hBN powder and nitrogen gas were used as B and N sources. The source materials were soaked at 1525 °C for 6 h, followed by subsequent cooling at a slow rate of 4 °C/h until solvent solidification. The slow cooling rate was employed to insure the precipitation of high quality crystals. Detailed growth conditions were discussed elsewhere.<sup>24</sup> The inset (a) of Fig. 1 shows an optical image of a bulk crystal of

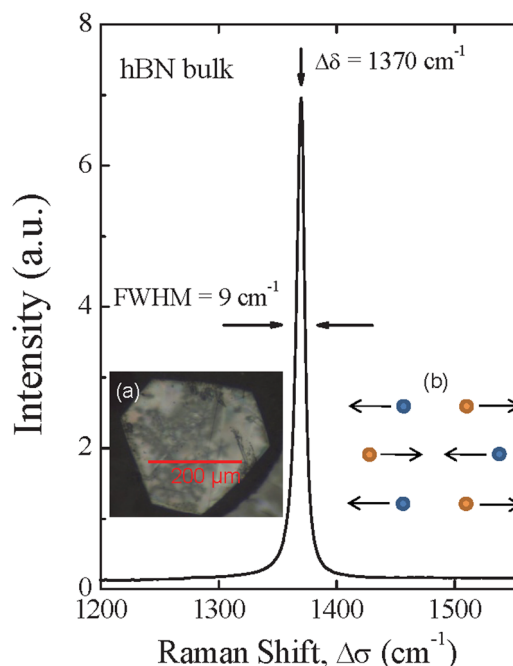


FIG. 1. Raman spectrum of a bulk hBN crystal using 780 nm excitation showing a peak at 1370  $\text{cm}^{-1}$  with a FWHM of 9  $\text{cm}^{-1}$ . Inset (a) is an optical image of the hBN bulk crystal used in this study and (b) is a schematic illustrating the in-plane vibrational stretch mode for the 1370  $\text{cm}^{-1}$  Raman line.

a)hx.jiang@ttu.edu

b)jingyu.lin@ttu.edu

hBN on Ni/Cr substrate having a dimension of about  $250\ \mu\text{m}$  across and  $30\ \mu\text{m}$  thick.

Raman spectra of hBN bulk crystals were measured using a Bruker Optics system and 780 nm excitation. A DUV time-resolved PL system was utilized to probe the emission properties.<sup>19</sup> The system consists of a frequency quadrupled 100 fs Ti:sapphire laser with excitation photon energy set around 6.28 eV and a monochromator (1.3 m) in conjunction with a single photon counting detection system (20 ps time-resolution) and a streak camera system (2 ps time-resolution). Figure 1 shows a typical Raman spectrum of hBN bulk crystals. The mode at  $\Delta\sigma = 1370\ \text{cm}^{-1}$  is attributed to the  $E_{2g}$  symmetry vibration in hBN, corresponding to the in-plane stretch of B and N atoms as illustrated in the inset (b) of Fig. 1.<sup>11,25</sup> The full-width-at-half-maximum (FWHM) of this Raman line is  $9\ \text{cm}^{-1}$ , which is among the smallest values reported in the literatures.<sup>11,25</sup> In Fig. 2, we present low temperature (10 K) band-edge PL emission spectrum of an hBN bulk crystal plotted in the region from 5.70 to 5.95 eV, where fine features are clearly resolved. The spectral line shape, including the spectral peak positions and the energy separations between the fine features, is very similar to the sharp exciton emission lines (so called S-series lines) previously observed in hBN crystals synthesized by high temperature and high pressure (HT-HP) techniques<sup>8</sup> and also in hBN powders.<sup>26</sup> The four main emission peaks located at 5.771 (S4), 5.799 (S3), 5.869 (S2), and 5.897 (S1) eV were attributed to the four Frenkel class free exciton levels originated from the doubly degenerated dipole-forbidden (dark) and dipole-allowed (bright) exciton states, in which the dark exciton state becomes allowed either due to the spontaneous symmetry breaking caused by energy transfer from bright exciton band as a result of the zero-point vibration of the lattice<sup>27,28</sup> or a strong spin-orbital interaction due to 2D layered structure.<sup>29</sup>

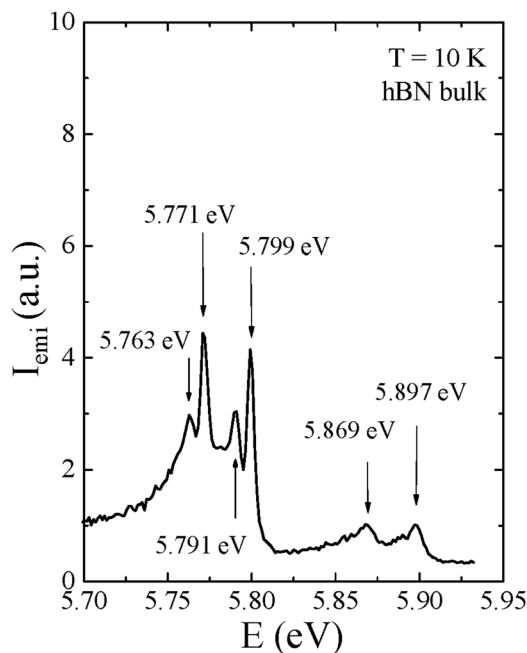


FIG. 2. Low temperature (10 K) band-edge PL spectrum of a bulk hBN crystal showing the S-series excitonic emission lines.

For 2D excitons, Paraskevov<sup>30</sup> suggests that because of the momentum conservation light emission resulting from direct exciton recombination in directions other than that of in-plane is induced by the exciton-acoustic phonon interaction. Based on this concept, the dependence of the exciton radiative lifetime  $\tau_R$  on the effective temperature of the exciton system was derived. The theory is generally valid when exciton-exciton interaction is negligibly small, i.e., the deBroglie wavelength of an exciton is much larger than the exciton Bohr radius. At  $T > T^*$ , the theory indicated that the function  $\tau_R(T)$  exhibits a well-known linear dependence. At  $T = T^*$ , the theory predicated that the lifetime  $\tau_R$  reaches its minimal value and at  $T < T^*$ , it increases with decreasing  $T$ . The characteristic temperature  $T^*$  is defined as

$$T^* = \hbar s / k a_B, \quad (1)$$

where  $\hbar = h/2\pi$  with  $h$  being the Planck's constant,  $s$  the sound velocity in the 2D layer,  $k$  the Boltzmann constant, and  $a_B$  the exciton Bohr radius. In typical semiconductors,  $T^*$  is quite low. For example,  $T^* \approx 3.6\ \text{K}$ , in GaAs quantum well.<sup>30</sup> Therefore, one typically observes the well-known linear dependence of  $\tau_R(T) \propto T$ . However, the S-series emission lines in hBN are attributed to the recombination of Frenkel excitons.<sup>26-29</sup> The Bohr radius of a Frenkel exciton is expected to be a few lattice constants. As such, the interaction between Frenkel excitons in hBN are expected to occur at a much higher density than the one in GaAs and is expected to be negligibly small under our experimental conditions. Though the spatial extend of Frenkel excitons is small, they travel as a wave throughout the crystal to provide an avenue to transfer energy from one point to another in the crystal.<sup>31,32</sup> We thus expect Eq. (1) to be applicable and may be demonstrated in hBN.

The PL decay kinetics of the S-series transitions has been measured at different temperatures. Figure 3(a) presents the PL decay characteristics of the main transition line (S4, 5.771 eV) measured at different temperatures ( $T$ ). The observed decay kinetics is slightly non-single exponential at intermediate temperatures, which may be due to the presence of the secondary peak at 5.763 (S4t). Due to the small energy difference between S4 and S4t, coupling between these two states may occur, which will contribute to the non-single exponential decay behavior. Due to the fact the PL decay is not a simple exponential, we measured the effective decay lifetime ( $\tau_{\text{eff}}$ ) of S4 line as a function of  $T$ , where  $\tau_{\text{eff}}$  is the time it takes the emission intensity to decay from its maximum value  $A$  to  $A/e$ . Figure 3(b) shows the overall  $T$  dependence of  $\tau_{\text{eff}}$ . If we assume the measured  $\tau_{\text{eff}}$  is dominated by the radiative recombination due the very large oscillator strength of excitons in hBN,<sup>27-29</sup> we then obtain experimentally a value of  $T^* \sim 175 (\pm 15)\ \text{K}$ , which is about 50 times higher than that in GaAs ( $T^* \approx 3.6\ \text{K}$  in GaAs), in which  $a_B \sim 10\ \text{nm}$ . The calculated sound velocity of longitudinal wave ( $p$ -wave) in hBN is about  $2.2 \times 10^6\ \text{cm/s}$ ,<sup>33</sup> which is about 4 times larger than that in GaAs. Using these data, we can deduce a value of exciton Bohr radius in hBN through

$$a_B(\text{hBN}) = \hbar s / 2\pi T^* \approx (4/50) a_B(\text{GaAs}) \approx 8\ \text{\AA}, \quad (2)$$

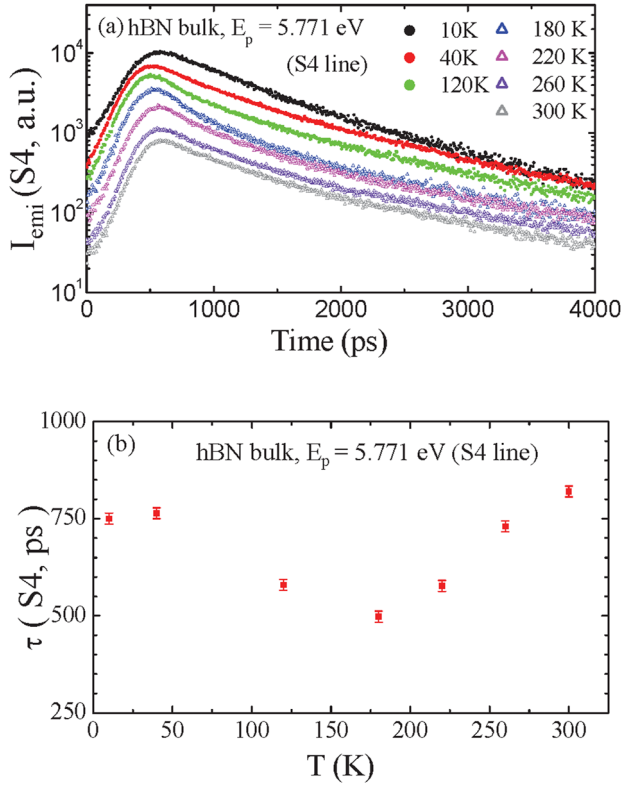


FIG. 3. Temperature dependence of the (a) PL decay characteristics and (b) effective decay-lifetime ( $\tau_{\text{eff}}$ ) of the S4 exciton emission line.

where we take  $a_B(\text{GaAs}) \approx 10 \text{ nm}$ . So the spatial extent of exciton in hBN spreads over  $\sim 3$  in-plane lattice constants, which is consistent with the picture that excitons in perfect hBN crystals belongs to a Frenkel class. From the value of  $a_B$ , we can estimate the binding energy of exciton in hBN using

$$E_B = \hbar^2 / (\pi^2 \mu a_B^2), \quad (3)$$

where the exciton reduced mass  $\mu = \epsilon m_o a_o / a_B$ ,  $a_o = 0.53 \text{ \AA}$  is the Bohr radius of hydrogen atom, and  $m_o$  is the mass of free electron. The measured in-plane dielectric constant of hBN is around  $\epsilon = 4$  (Ref. 34), and we therefore obtain a value of  $E_B \approx 740 \text{ meV}$  and minimum direct band gap of about  $6.51 \text{ eV}$ . Our estimated values agree quite well with the calculated values of  $E_B \approx 720 \text{ meV}$  and a minimum direct band gap of about  $6.47 \text{ eV}$ .<sup>27</sup> The reduced mass of 2D exciton in hBN can also be obtained directly from the measured value of the Bohr radius,  $\mu = \epsilon m_o a_o / a_B \approx 0.27 m_o$ .

One could also estimate the reduced mass of 2D exciton in hBN from the dispersion relation of single sheet hBN derived from a tight-binding model<sup>35,36</sup>

$$E^2(\mathbf{k}) = \beta^2 + t^2 [3 + 2 \text{Cos}(3^{1/2} k_y a) + 4 \text{Cos}(3^{1/2} k_y a / 2) \text{Cos}(3 k_x a / 2)], \quad (4)$$

where  $\beta$  is the energy difference of electron localized on B and N atoms for hBN and  $t$  is the nearest-neighbor hopping energy ( $2.8\text{--}3.1 \text{ eV}$  in graphene) and  $a$  is the in-plane boron-nitrogen ( $1.446 \text{ \AA}$ ) or carbon-carbon ( $1.42 \text{ \AA}$ ) distance. Expanding Eq. (4) near the Dirac points  $\mathbf{K}$  and  $\mathbf{K}'$ , we have

$$E(\mathbf{q}) = \pm [\beta^2 + v_f^2 \hbar^2 q^2]^{1/2} = \pm [\beta^2 + (3ta/2\hbar)^2 \hbar^2 q^2]^{1/2}, \quad (5)$$

where “+” sign is for electrons and “−” sign for holes. Similar to graphene, we have exactly the same dispersion relation for the electrons and holes in single sheet hBN. In this regard, holes are truly anti-particles of electrons in single sheet hBN. At the Dirac points,  $q=0$ , the minimum (maximum) energy of the conduction (valance) band is  $E_{\text{min}}^c = +\beta$  ( $E_{\text{max}}^v = -\beta$ ) and thus  $E_g = 2\beta$ . It is clear that a single sheet hBN is a direct bandgap material with an energy bandgap of  $2\beta$ . By comparing Eq. (5) with the relation for relativistic particles, we have

$$E^2(\mathbf{q}) = (m_a v_f^2)^2 + (\hbar v_f q)^2, \quad (6)$$

$v_f = 3ta/2\hbar$ ,  $\beta = m_a v_f^2$ , and  $m_a = 1/2(2\hbar/3ta)^2 E_g$ . It is interesting to note that Eq. (6) represents the generalized dispersion relation of 2D systems, which provides a direct relationship between the effective mass ( $m_a$ ) and bandgap ( $E_g$ ). The parameter  $t$  in hBN is similar to that in graphene. Using  $E_g (= 2\beta) \approx 6.0 \text{ eV}$  and  $t \approx 3 \text{ eV}$  for hBN, we obtain the effective masses of electrons and holes in single sheet hBN to be around  $0.54 m_o$ . This implies that the reduced mass of 2D excitons in hBN is around  $\mu \approx 0.27 m_o$ , which is remarkably close to the value deduced from 2D exciton Bohr radius obtained from experimentally measured T dependence of the exciton decay lifetime (Fig. 3(b)). Our experimentally deduced value of electron and hole effective mass in hBN is also very close to the calculated effective mass of  $0.5 m_o$ .<sup>37,38</sup> This further suggests that excitons in 3D hBN crystals possess 2D characters. We would like to emphasize that the evidence for the 2D exciton character in 3D hBN is not solely based on the time-resolved PL measurement results but also comes from the overall coincidence of all possible hints, experimental data, and calculations.

In summary, the theory for 2D exciton recombination<sup>30</sup> seems to adequately describe the exciton dynamics in 3D hBN. The exciton Bohr radius and exciton binding energy deduced from the temperature dependent exciton recombination lifetime is around  $8 \text{ \AA}$  and  $740 \text{ meV}$ , respectively. The deduced 2D exciton reduced mass ( $\mu \approx 0.27 m_o$ ) is consistent with that derived from the relativistic dispersion relation of hBN single sheet which provides the effective masses of electrons and holes in single sheet hBN to be around  $0.54 m_o$ . We thus believe that the 2D nature hBN provides a very unique platform to study the properties of relativistic particles; positronium in particular, in 2D condensed matter systems. Following the isolation of graphene,<sup>39</sup> intensive research activities are currently undertaken worldwide in the areas beyond graphene—2D materials having non-zero energy band gaps. The generalized dispersion relation for 2D systems derived from a tight-binding model<sup>35,36</sup> is expected to be applicable to different 2D material systems.

The effort on the optical studies of hBN was supported by DOE (Grant No. FG02-09ER46552) and the effort of bulk hBN crystal growth was supported by DHS ARI Program (Grant No. 2011-DN-077-ARI048). Jiang and Lin

are grateful to Dr. Su-Huai Wei and Dr. Bing Huang for insightful discussion and to the AT&T Foundation for the support of Ed Whitacre and Linda Whitacre endowed chairs.

- <sup>1</sup>S. L. Rumyantsev, M. E. Levinshtein, A. D. Jackson, S. N. Mohammad, G. L. Harris, M. G. Spencer, and M. S. Shur, in *Properties of Advanced Semiconductor Materials GaN, AlN, InN, BN, SiC, SiGe*, edited by M. E. Levinshtein, S. L. Rumyantsev, and M. S. Shur (John Wiley & Sons, Inc., New York, 2001), pp. 67–92.
- <sup>2</sup>Y. Kubota, K. Watanabe, O. Tsuda, and T. Taniguchi, *Science* **317**, 932 (2007).
- <sup>3</sup>T. Sugino, K. Tanioka, S. Kawasaki, and J. Shirafuji, *Jpn. J. Appl. Phys. Part 2* **36**, L463 (1997).
- <sup>4</sup>J. Li, R. Dahal, S. Majety, J. Y. Lin, and H. X. Jiang, *Nucl. Instrum. Methods Phys. Res. A* **654**, 417 (2011).
- <sup>5</sup>K. Watanabe, T. Taniguchi, and H. Kanda, *Nature Photonics* **3**, 591 (2009).
- <sup>6</sup>T. Taniguchi and K. Watanabe, *J. Cryst. Growth* **303**, 525 (2007).
- <sup>7</sup>K. Watanabe, T. Taniguchi, T. Kuroda, O. Tsuda, and H. Kanda, *Diamond Relat. Mater.* **17**, 830 (2008).
- <sup>8</sup>K. Watanabe and T. Taniguchi, *Phys. Rev. B* **79**, 193104 (2009).
- <sup>9</sup>K. Watanabe and T. Taniguchi, *Int. J. Appl. Ceram. Technol.* **8**, 977 (2011).
- <sup>10</sup>L. Song, L. Ci, H. Lu, P. B. Sorokin, C. Jin, J. Ni, A. G. Kvashnin, D. G. Kvashnin, J. Lou, B. I. Yakobson, and P. M. Ajayan, *Nano Lett.* **10**, 3209 (2010).
- <sup>11</sup>R. V. Gorbachev, I. Riaz, R. R. Nair, R. Jalil, L. Britnell, B. D. Belle, E. W. Hill, K. S. Novoselov, K. Watanabe, T. Taniguchi, A. K. Geim, and P. Blake, *Small* **7**, 465 (2011).
- <sup>12</sup>Y. Shi, C. Hamsen, X. Jia, K. K. Kim, A. Reina, M. Hofmann, A. L. Hsu, K. Zhang, H. Li, Z. Y. Juang, M. S. Dresselhaus, L. J. Li, and J. Kong, *Nano Lett.* **10**, 4134 (2010).
- <sup>13</sup>N. Alem, R. Erni, C. Kisielowski, M. D. Rossell, W. Gannett, and A. Zettl, *Phys. Rev. B* **80**, 155425 (2009).
- <sup>14</sup>C. R. Dean, A. F. Young, I. Meric, C. Lee, L. Wang, S. Sorgenfrei, K. Watanabe, T. Taniguchi, P. Kim, K. L. Shepard, and J. Hone, *Nat. Nanotechnol.* **5**, 722 (2010).
- <sup>15</sup>L. Britnell, R. V. Gorbachev, R. Jalil, B. D. Belle, F. Schedin, A. Mishchenko, T. Georgiou, M. I. Katsnelson, L. Eaves, S. V. Morozov, N. M. R. Peres, J. Leist, A. K. Geim, K. S. Novoselov, and L. A. Ponomarenko, *Science* **335**, 947 (2012).
- <sup>16</sup>C. Dean, A. F. Young, L. Wang, I. Meric, G.-H. Lee, K. Watanabe, T. Taniguchi, K. Shepard, P. Kim, and J. Hone, *Solid State Commun.* **152**, 1275 (2012).
- <sup>17</sup>A. K. Geim and I. V. Grigorieva, *Nature* **499**, 419 (2013).
- <sup>18</sup>R. Dahal, J. Li, S. Majety, B. N. Pantha, X. K. Cao, J. Y. Lin, and H. X. Jiang, *Appl. Phys. Lett.* **98**, 211110 (2011).
- <sup>19</sup>S. Majety, X. K. Cao, J. Li, R. Dahal, J. Y. Lin, and H. X. Jiang, *Appl. Phys. Lett.* **101**, 051110 (2012).
- <sup>20</sup>S. Majety, J. Li, X. K. Cao, R. Dahal, B. N. Pantha, J. Y. Lin, and H. X. Jiang, *Appl. Phys. Lett.* **100**, 061121 (2012).
- <sup>21</sup>J. Li, S. Majety, R. Dahal, W. P. Zhao, J. Y. Lin, and H. X. Jiang, *Appl. Phys. Lett.* **101**, 171112 (2012).
- <sup>22</sup>B. Huang, X. K. Cao, H. X. Jiang, J. Y. Lin, and S. H. Wei, *Phys. Rev. B* **86**, 155202 (2012).
- <sup>23</sup>Y. Kubota, K. Watanabe, O. Tsuda, and T. Taniguchi, *Chem. Mater.* **20**, 1661 (2008).
- <sup>24</sup>B. Clubine, M.S. thesis, Kansan State University, 2012.
- <sup>25</sup>R. J. Nemanich, S. A. Solin, and R. M. Martin, *Phys. Rev. B* **23**, 6348 (1981).
- <sup>26</sup>P. Jaffrennou, J. Barjon, J.-S. Lauret, B. Attal-Trétout, F. Ducastelle, and A. Loiseau, *J. Appl. Phys.* **102**, 116102 (2007).
- <sup>27</sup>B. Arnaud, S. Lebègue, P. Rabiller, and M. Alouani, *Phys. Rev. Lett.* **96**, 026402 (2006).
- <sup>28</sup>B. Arnaud, S. Lebègue, P. Rabiller, and M. Alouani, *Phys. Rev. Lett.* **100**, 189702 (2008).
- <sup>29</sup>L. Wirtz, A. Marini, and A. Rubio, *Phys. Rev. Lett.* **96**, 126104 (2006).
- <sup>30</sup>A. V. Paraskevov, *J. Lumin.* **132**, 2913 (2012).
- <sup>31</sup>G. D. Mahan, *Condensed Matter in a Nutshell* (Princeton University Press, Princeton, New Jersey, 2011), p. 12.
- <sup>32</sup>P. K. Basu, *Theory of Optical Processes in Semiconductors: Bulk and Microstructures* (Oxford University Press, Oxford, 1997), p. 124.
- <sup>33</sup>Q. Peng, A. R. Zamiri, W. Ji, and S. De, *Acta Mech.* **223**, 2591 (2012).
- <sup>34</sup>A. J. Gatesman, R. H. Giles, and J. Waldman, 1991 MRS Fall Meeting, Symposium G – Wide Band-Gap Semiconductors (Mater. Res. Soc. Symp. Proc., 1992), Vol. 242, p. 623.
- <sup>35</sup>P. R. Wallace, *Phys. Rev.* **71**, 622 (1947).
- <sup>36</sup>G. W. Semenoff, *Phys. Rev. Lett.* **53**, 2449 (1984).
- <sup>37</sup>L. Britnell, R. V. Gorbachev, R. Jalil, B. D. Belle, F. Schedin, M. I. Katsnelson, L. Eaves, S. V. Morozov, A. S. Mayorov, N. M. R. Peres, A. H. C. Neto, J. Leist, A. K. Geim, L. A. Ponomarenko, and K. S. Novoselov, *Nano Lett.* **12**, 1707 (2012).
- <sup>38</sup>Y. N. Xu and W. T. Ching, *Phys. Rev. B* **44**, 7787 (1991).
- <sup>39</sup>A. K. Geim and K. S. Novoselov, *Nature Mater.* **6**, 183 (2007).